Infrared Reflection–Absorption Spectroscopy and Polarization-Modulated Infrared Reflection–Absorption Spectroscopy Studies of the Organophosphorus Acid Anhydrolase Langmuir Monolay…

ARTICLE *in* THE JOURNAL OF PHYSICAL CHEMISTRY B · MAY 2008

Impact Factor: 3.3 · DOI: 10.1021/jp709591e · Source: PubMed

Secondary Structure of Organophosphorus Hydrolase in Solution and in Langmuir−Blodgett Film Studied by Circular Dichroism Spectroscopy

Jiayin Zheng,[†] Celeste A. Constantine,[†] Vipin K. Rastogi,[‡] Tu-Chen Cheng,[§] Joseph J. DeFrank,[‡] and Roger M. Leblanc*,[†]

Department of Chemistry, University of Miami, Coral Gables, Florida 33124-0431, U.S. Army Edgewood Chemical & Biological Center, Aberdeen Proving Ground, Maryland 21010-5423, and GEO-Centers, Inc., Gunpowder Club, Aberdeen Proving Ground, Maryland 21010

Received: May 25, 2004; In Final Form: September 1, 2004

The secondary structure of organophosphorus hydrolase (OPH) has been studied with circular dichroism (CD) spectroscopy in the far-UV region. The effect of pH on the secondary structure of OPH solution was examined over the pH range from 3.56 to 9.60. As shown on the CD spectra, the secondary structure of OPH is well defined when the pH value is near the isoelectric point (7.6); however, it is destroyed when the pH values are increased or decreased further. This is explained by the loss of helical structure. The pH effect on CD spectra contributes to clarify the optimum pH needed to obtain a stable OPH Langmuir film at the air−water interface and its correlation to the secondary structure of the enzyme. Comparative study of the thermal treatment on the secondary structure of OPH in solution, Langmuir−Blodgett film, and dry film shows that the molecular arrangement plays a dominant role in the thermal stability of OPH. With use of the CDPro software package a quantitative estimation of the secondary structure from the CD spectra of OPH solution was obtained. Results show that there is a decrease in the percentage of the α-helical and an increase of β-strands with the change of pH or temperature.

Introduction

Organophosphorus (OP) compounds are esters, amides, or thiol derivatives of phosphonic acid and form a large family (>50 000 compounds) of insecticides and chemical warfare (CW) agents. However, they are also a major global cause of health problems.[1] When ingested, inhaled, or absorbed through the skin, these compounds inhibit acetylcholinesterase, which transmits nerve impulses across synaptic junctions. Due to their critical consequences, there is a need for improving sensors or techniques to detect organophosphates in the air, soil, and water, as well as in food.[2] Enzyme-based biosensors have been explored for environmental monitoring of OPs since they have a rapid response time and are sensitive. Organophosphorus hydrolase (OPH) has the ability to catalyze the hydrolysis of a wide range of OP pesticides such as paraoxon, parathion, coumaphos, diazinon, dursban, methyl parathion, etc., and CW agents, such as sarin and soman.[3−6] OPH-based biosensor assays respond to OP compounds as enzyme substrates directly rather than inhibitors or antigens. Consequently, these assays can be reversible and require only the analyte of interest and showed considerable potential in biosensor applications.[7]

To develop OPH-based biosensors, the studies on the organization of OPH at interfaces and after immobilization have been initiated.[8] The layer-by-layer (LBL)[9−11] and Langmuir−Blodgett (LB) film deposition techniques are two major immobilization methods for OPH. They have potential industrial applications in the development of biosensors because well-ordered, stable films with high strength are formed.[12−14] The unique native fold of an enzyme is crucial to its activity. Therefore, upon immobilization, the enzyme conformation must be maintained for optimal performance of the biosensor. There are several factors which affect the activity of enzymes. Under certain environmental conditions such as pH and temperature, enzymes become misfolded. Since the enzyme activity depends on its native secondary structure characteristics, it is very important to study the enzyme conformation changes of OPH with respect to environmental factors such as pH and temperature.

A detailed surface chemistry study of OPH at the air−water interface has already been reported by Cao et al.[15] It revealed the necessity of an optimal experimental condition, namely pH 7.6 and 0.5 M KCl concentration in the subphase. This experimental condition is essential for obtaining a homogeneous and stable Langmuir monolayer. To explore the structure of OPH under these conditions, circular dichroism (CD), a well−known excellent spectroscopic technique to obtain information on the secondary structure of enzymes, has been employed. Enzymes give distinctive CD spectra in the far-UV, typically between 180 and 250 nm. This corresponds to electronic transitions of the backbone chromophore of the enzyme. From the CD spectra it is possible to determine the approximate proportion of the different elements of secondary structure (α-helices and β-strands) in the enzyme.[16−20] Recently, CD has been widely used to analyze the main properties and features of enzyme solutions and films,[21−24] which show a bright future for this spectroscopic technique in biosensor research.

There are three popular methods (SELCON3, CONTIN, CDSSTR) for estimating protein secondary structure fractions from CD spectra.[17,25−28] But it is also difficult to compare the results from different methods because of the different reference

* To whom correspondence should be addressed. Phone: (305) 284-2194. Fax: (305) 284-6367. E-mail: rml@miami.edu.
[†] University of Miami.
[‡] U.S. Army Edgewood Chemical & Biological Center.
[§] GEO-Centers, Inc.

10.1021/jp0477396 CCC: $27.50
Published on Web 10/13/2004

sets and different secondary structure assignments used in those methods of analysis.[17] The CDPro software package consists of these three programs and a program for determining tertiary structure class (CLUSTER). One of the major advantages of the CDPro software package is that the programs have been modified to accept any given set of reference proteins (CD spectra and secondary structure fractions), and seven such reference sets are provided. Moreover, input data files for these three programs are identical. More information about CDPro is available at the following website: http://lamar.colostate.edu/~sreeram/CDPro. The assignment from CDPro gave six secondary structural classes: regular α-helix, α_R; distorted α-helix, α_D; regular β-strand, β_R; distorted β-strand, β_D; turns, T; and unordered, U.

In this paper, the effect of pH and temperature on the conformation of OPH was examined by using the CD spectroscopic technique. Comparative studies of the thermal effect on the secondary structure of OPH for three different types of samples, namely solution, LB film, and dry film, were performed to determine the stability of the OPH secondary structure in different phases.

Experimental Section

Materials. Purified OPH (E. C.3.1.8.1) was obtained from the U.S. Army Laboratory (Edgewood Chemical and Biological Center, APG, MD) with a purity of 85−90%. OPH stock solution (0.3 mg/mL) was prepared in 100 mM bis-tris-propane (BTP), pH 7.5, containing 10 μM Co^{2+}. The stock solution was kept in the refrigerator at 4 °C.

The solution for OPH LB film preparation and for CD measurements was freshly made on the day of the experiment at a concentration of 0.075 mg/mL. The water used as a subphase was purified by a Modulab 2020 water purification system (Continental Water Systems Corp., San Antonio, TX). The pure water has a specific resistance of 18 MΩ·cm and a surface tension of 72.6 mN m^{-1} at 20 ± 1 °C. A buffer solution with a pH value of 7.5 (0.1 M KH_2PO_4 and 0.1 M NaOH) was used as spreading solvent and as subphase. KCl was added into the buffer solution as an electrolyte. All the chemicals were purchased from Sigma Chemical Co. (St. Louis, MO).

Methods. Experiments were designed to determine the optimum conditions for developing a stable monolayer of OPH at the air−water interface and the stability of this monolayer was examined by the compression/decompression cycle. Detailed experimental conditions were described in ref 15.

The secondary structure of OPH was determined with a Jasco J-810 spectropolarimeter fitted with a 150-W xenon lamp. Quartz cells of 1-mm path length were used for all CD measurements of OPH solution, and the spectra were recorded in the far-UV region (185−260 nm) with a response time of 8 s and scan speed of 50 nm/min. Three scans were accumulated and averaged for each spectrum after the background of the buffer solution or blank quartz slide was subtracted.

Measurements of the pH effect on the secondary structure of OPH were done in 100 mM BTP buffer, pH 7.5, in the presence of 10 μM Co^{2+}. pH titration was started from pH 7.6, then the OPH solution was titrated to pH 3.56 and 9.6 by the addition of 1.0 M HCL and 1.0 M NaOH, respectively. During titration, the pH value was monitored with a Pinnacle 545 pH meter. The spectrum of OPH at each pH was recorded 5 min after each change of pH to allow equilibration.

The surface chemistry experiments were done in a clean room class 1000, with a constant temperature of 20.0 ± 0.5 °C and a relative humidity of 50 ± 1%. A μ-S trough (Kibron Inc. Fin

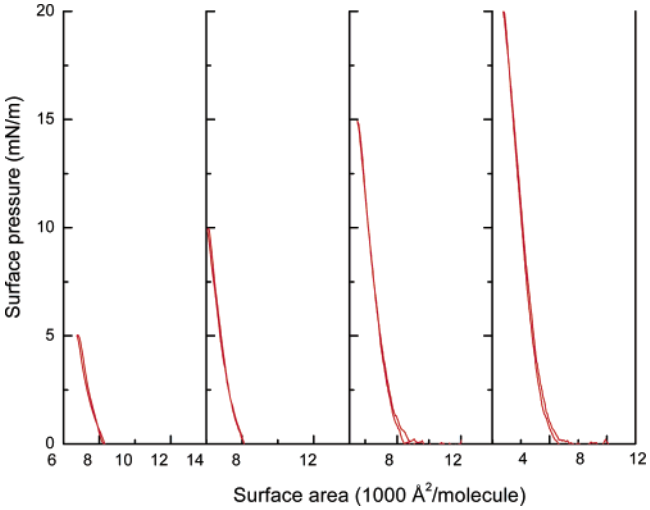

Figure 1. The compression/decompression cycle of OPH monolayer at pH 7.6 buffer subphase in the presence of 0.5 M KCl from nil to 5, 10, 15, and 20 mN/m surface pressure.

00171, Helsinki, Finland) with an area of 115 cm^2 (5.9 cm × 19.5 cm) was utilized. This trough had a centrally located cavity for LB film deposition. The trough was supplied with a Wilhelmy plate wire probe that had a sensitivity of 0.02 mN m^{-1}. For fabrication of OPH LB film, the quartz slides were cleaned by first dipping them in an ultrasonic bath containing a detergent solution for 20 min to thoroughly remove the impurities from the slide surfaces. An additional 30 min of sonication in deionized water was conducted to eliminate detergent residue. This was followed by drying the slides in an oven for 1 h. Activation of the quartz slides was carried out by dipping the clean slides into 0.4 g/L of octadecyltrichlorosilane (OTS) solution in cyclohexane for 30 min (with stirring). The hydrophobic slides were sonicated in cyclohexane to remove the excess of OTS and stored under cyclohexane prior to use.

The monolayers were transferred onto the surface of the hydrophobic quartz slides by the Langmuir−Blodgett film technique. The subphase for LB film deposition is the same as the Langmuir film preparation. The deposition ratio was near unity and 30 layers were deposited on the slide. The OPH-LB film was placed manually, perpendicular to the light path inside the spectropolarimeter. Dry films of OPH were deposited by spreading the OPH solutions (0.2 mg/mL) over the hydrophobic quartz slide and dried in the nitrogen flux. Thermal treatment of the samples was performed by heating the samples directly inside the spectropolarimeter after it was connected to a circulating water bath.

Results and Discussion

The surface pressure−area isotherm of OPH was discussed thoroughly in our previous work.[15] It revealed that a pH 7.6 subphase (composed of 0.1 M KH_2PO_4, 0.1 M NaOH, and containing 0.5 M KCl) produced a stable and homogeneous OPH monolayer at the air−water interface. The stability of the OPH monolayer at the air−water interface was examined by the compression/decompression cycle under the optimal conditions of the subphase, and the result is shown in Figure 1. No significant decrease in the apparent limiting molecular area was observed during the compression and decompression cycles at surface pressures of 5, 10, 15, and 20 mN m^{-1}. This suggests the formation of a stable OPH monolayer under those surface pressures at the air−water interface.

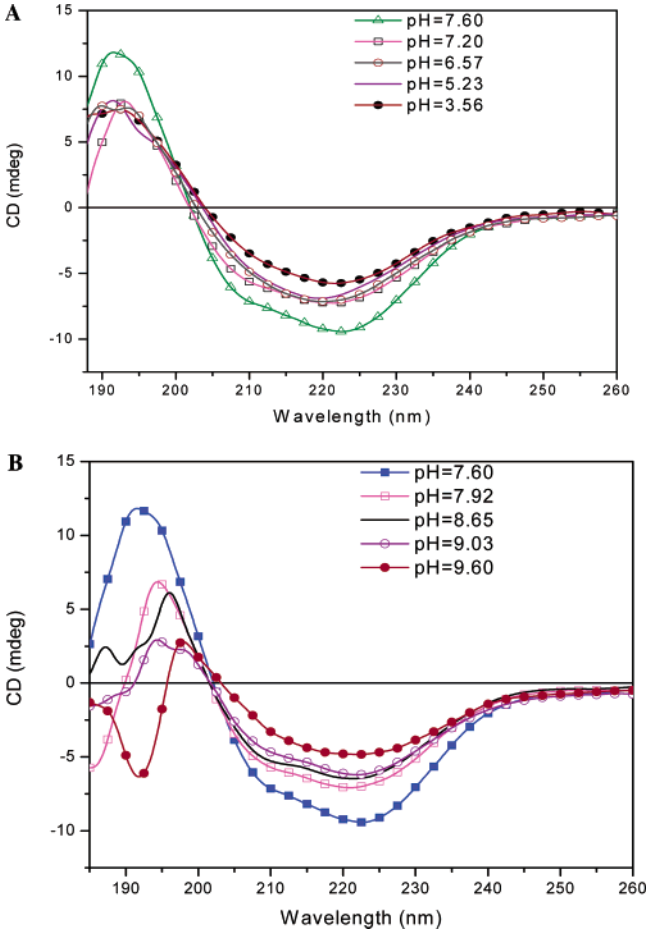

Figure 2. pH effect on CD spectra of OPH solution (0.075 mg/mL) from pH 7.60 to 3.56 (A) and pH 7.60 to 9.60 (B).

TABLE 1: The Average Estimation of Secondary Structure Fractions of OPH Solution with the CDPro Software Package under Different Temperatures and pH Values[a]

	fraction of secondary structure, %					
	α_R	α_D	β_R	β_D	T	U
OPH solution (20 °C)						
pH 7.60	36.7	26.5	3.4	5.1	12.0	16.4
pH 3.56	24.8	18.4	10.3	12.5	20.1	14.7
pH 9.60	21.3	17.0	10.1	14.5	18.0	20.0
OPH solution 40 °C	25.8	19.2	8.7	10.0	14.6	22.0
OPH solution 60 °C	12.4	13.3	10.8	18.3	20.9	24.9

[a] α_R, regular α-helix; α_D, distorted α-helix; β_R, regular β-strand; β_D, distorted β-strand; T, turns; and U, unordered.

Figure 2 shows the pH-dependent change on the secondary structure of OPH solution below and above the isoelectric point of OPH, i.e., pH 7.6.[29] At pH 7.6, the spectrum showed a double peak typical of high α-helical content. The variation of pH led to a change in the intensity and shape of the CD spectrum, dramatically reducing the contribution of the two negative α-helix peaks. For example, when the pH was reduced to 3.56, the two negative peaks became a broad negative peak on the CD spectrum, which is more similar to that of the β-rich structure. Table 1 shows the average fraction of the secondary structure estimated from the CD data obtained with the CDPro software package. The regular α-helix content was 36.7% and the distorted α-helix content was 26.5% at pH 7.60 while the two helix structures were reduced to 24.8% and 18.4% when the pH reached 3.24, respectively. When the pH reached 9.60, the two structures were reduced to 21.3% and 17.0%, respectively. At the same time, the visual observation of the sample

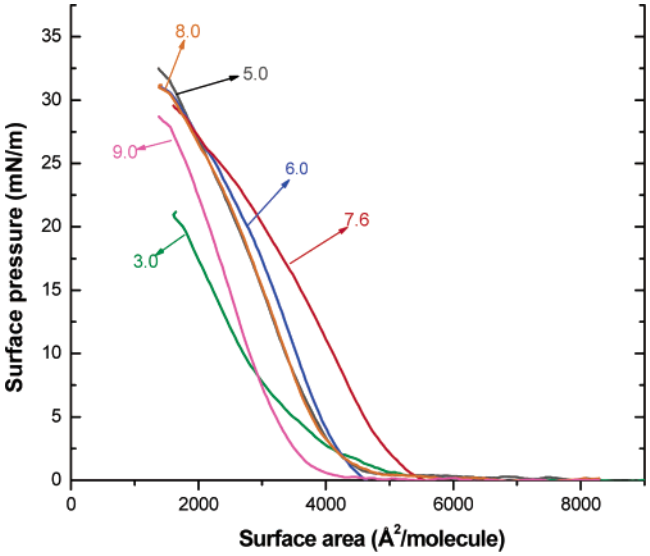

Figure 3. Surface pressure−area isotherms of the OPH monolayer obtained with different buffer subphases as different pH values, i.e., pH 3.0, 5.0, 6.0, 7.6, 8.0, and 9.0.

solution showed some turbidity when the pH changed from the isoelectric point to 3.56 or 9.60, which indicated an aggregation of the enzyme leading to an insoluble enzyme solution. The data in Table 1 also showed that there is a great increase in the two kinds of β-strand structures along with the change of the pH from the isoelectric point, indicating that the β-strand structure may be the more stable secondary structure than the α-helix when there is an aggregation of the enzyme.

The presence of an approximate isodichroic point at around 204 nm in both panels A and B of Figure 2 suggested that the aggregation of the enzyme could be approximated by a two-state model. For example, in Figure 2A, when the pH was decreased from 7.60 to 7.20, the enzyme still maintained some of the α-helix conformation. When the pH was further decreased to 3.56, the enzyme was almost fully aggregated as evidenced by a broad and very weak negative peak. In Figure 2B, the negative peak of 221 nm, which is assigned to the α-helix structure, was less obvious when the pH was changed slightly (from 7.60 to 7.92) and the intensity of the peak decreased significantly when the pH reached 9.60. Thus we confirmed that the secondary structure of the OPH solution is strongly affected by pH and the most stable secondary structure is obtained at a pH near the isoelectric point of the enzyme. The two most important factors affecting an enzyme's conformation are the amino acid sequence and the environmental conditions which include pH, temperature, and ionic strength.[21] When the pH of the OPH solution changes, the electrostatic interactions between charged amino acids are also changed, so that the enzyme molecules encounter a very different environment, hence cause a loss of the peak intensity and shape.

Another interesting observation about these results is their correlation with the pH effect on the OPH monolayer. The OPH $\pi-A$ isotherms at different pH values are shown in Figure 3. We can see that the pH of the subphase has a significant effect on the conformation of the enzyme. At pH 7.6, which is the isoelectric point of the enzyme, the OPH monolayer was compressed at nil surface pressure to a larger surface area per molecule and a lower collapse surface pressure than those obtained at the other pH values, which shows the isotherm of OPH under this pH represents the most stable and insoluble OPH monolayer at the air−water interface. This is because the presence of equal numbers of positive and negative charges

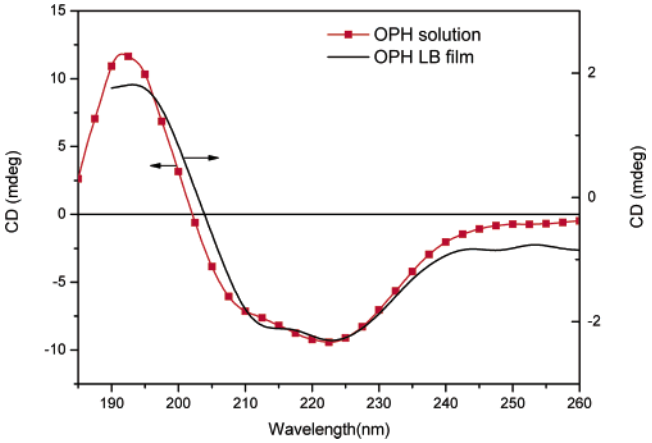

Figure 4. CD spectra of OPH solution (0.075 mg/mL) and LB film (30 layers).

facilitates favorable ionic interactions between enzyme molecules. The CD results explain this observed phenomenon. At pH 7.6 the CD spectrum gives the most defined secondary structure with the least amount of conformation change.

On the basis of the surface chemistry results above, we chose 20 mN m^{-1} as the optimal surface pressure for the LB deposition. The collapse surface pressure of the OPH monolayer was approximately 25 mN m^{-1}, therefore the surface pressure for LB deposition must be smaller than the collapse pressure to ensure the homogeneity of the Langmuir film. Moreover, the OPH monolayer is stable during the whole compression procedure up to 20 mN m^{-1} as shown in Figure 1. At this surface pressure, the enzyme at the air−water interface is closely packed. Consequently, a more well-organized LB film necessary for the CD measurements is obtained.

Figure 4 shows the CD spectra of OPH in solution and LB film. Both spectra showed two negative peaks near 210 and 221 nm, which were assigned to the α-helix structure. The crossover point at 203 nm and the positive peak at 191 nm were also assigned to the α-helix structure. The CD spectrum of the OPH LB film was in excellent agreement with positions observed for the conformation in solution, only the negative maxima shift slightly (from 210 and 221 nm to 213 and 223 nm). This difference may be within experimental error but could also arise from the steric interaction between the adsorbed enzyme and the hydrophobic surface after the film deposition. In the presence of the hydrophobic surface, there is some degree of conformational change due to refolding effects of the enzyme at the interface, in which the hydrophobic domains inside the enzyme become exposed to the surface. The typical double minimum of the α-helix was better defined in LB film than in solution. One conclusion from these data is that adsorbed OPH has the same or similar conformation to that in aqueous solution, but the hydrophobic surface may cause very minor CD spectroscopic changes.

CD spectra of different samples of OPH, i.e., solution, LB film, and dry film after heating at different temperatures, are presented in Figure 5. Figure 5A shows there is no significant change in the CD spectra when the temperature was increased from 20 to 35 °C. However, a progressive decrease in the intensity of the OPH CD signal in solution was observed when the temperature was increased from 35 to 50 °C, indicating a process of partial denaturation that corresponds to a steady decrease of α-helix conformation. When the temperature was raised to 55 and 60 °C, the two α-helix peaks were totally lost and became a wide and weak negative peak. The data in Table 1 show clearly that the regular and distorted α-helix structure

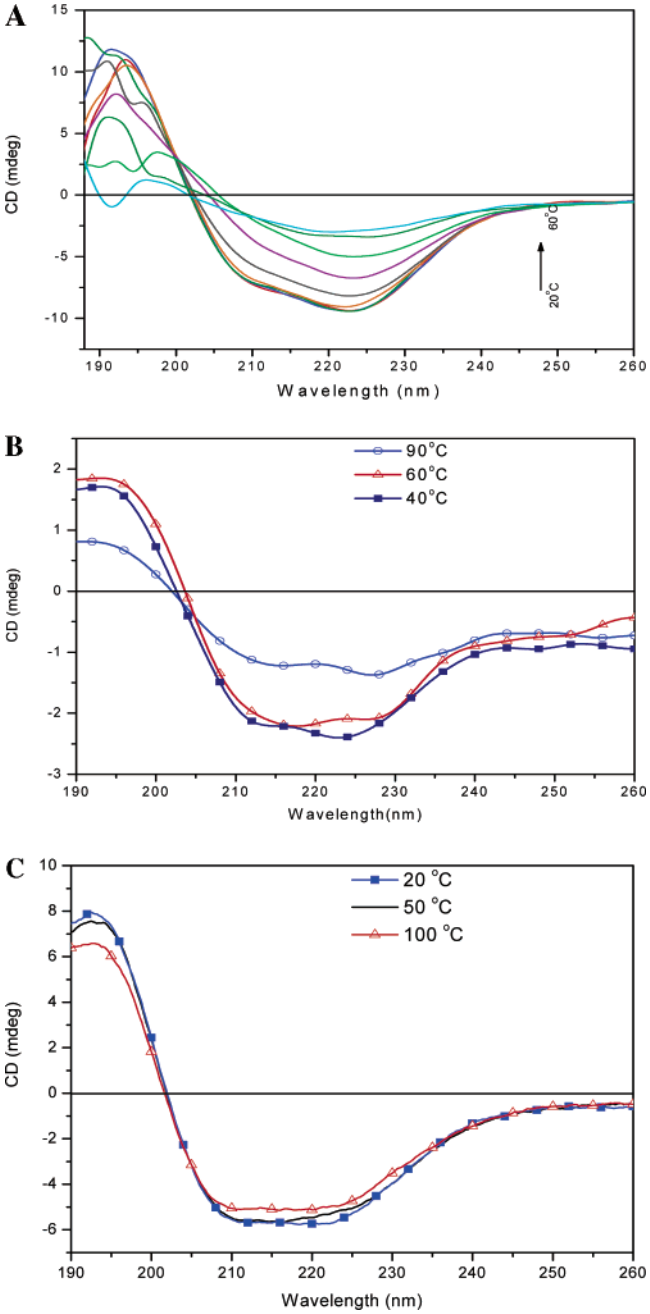

Figure 5. The effect of temperature on the CD spectra of OPH solution (0.075 mg/mL) from 20 to 60 °C (A), LB film at 40, 60, and 90 °C (30 layers) (B), and dry film at 20, 50, and 100 °C (C).

percentage decreased from 36.7% and 26.5% to 12.4% and 13.3% respectively when the temperature increased from 20 to 60 °C. Such phenomena occurred because in the α-helix conformation, intrachain H-bonding interactions play a significant role in maintaining the three-dimensional structure of the enzyme. An increase in temperature causes stronger motional fluctuations in H-bonds which disrupts this structure and leads to the enzyme denaturation. Also indicated in Table 1 was a relatively great increase in the percentage of both regular and distorted β-strand structure (from 3.4% and 5.1% to 10.8% and 18.3%) and a relatively large increase in the percentage of the unordered structure (16.4% to 24.9%). Generally, during the process of denaturation, the enzyme unfolds and the conformation associated with proper folding of the protein such as α-helix is compromised. This leads to a subsequent increase in the

percentage of β-strand, β-turn and the unordered secondary structure, so that the protein becomes insoluble.

Figure 5B shows the temperature effect of the OPH LB film. When the temperature was at 40 °C, there was a double minimum at 213 and 223 nm that was assigned to the α-helix structure. These two peaks shifted to 215 and 226 nm, respectively, when the temperature was raised to 60 °C, with similar intensity as 40 °C. There was a significant difference in peak intensity only after the temperature reached 90 °C, implying that the thermal stability of the OPH LB film was much higher than that of the OPH in solution.

CD spectra of the OPH dry film after heating at different temperatures are shown in Figure 5C. At room temperature, the two negative α-helix peaks of the dry film were not so apparent on the CD spectra of OPH and only two slight shoulders at 210 and 222 nm were observed. The difference in CD spectra between the OPH dry film and the LB film was probably due to the difference in their organization. LB films are well-organized, which leads to a corresponding well-defined secondary structure. Comparing panels C and A in Figure 5, there was only a small decrease in peak intensity of the α-helix structure of the OPH dry film after the temperature was increased to 100 °C.

In short, the OPH LB film and dry film are much more resistant to the temperature effect than OPH in solution. They both demonstrate high thermal stability. Here we support Erokhin et al.'s conclusion[22] that a close molecular packing of enzyme is the prime parameter responsible for the thermal stability. The OPH molecules are randomly distributed in solution, whereas the OPH molecules organize themselves when they are fabricated as a film. Therefore, immobilization of the enzyme increases its thermal stability.

Conclusion

The pH and temperature effects on the secondary structure of OPH were studied in this work and overall analysis of the OPH CD spectra has provided information on the structural changes involved when the environment was altered. Native OPH has a significant percentage of α-helix regions and the most stable secondary structure of OPH solution can be obtained at pH 7.6, which is also the isoelectric point of the enzyme. When the pH changes, the α-helix is converted into β-strand conformation and the enzyme becomes insoluble. Physical instability such as aggregation and/or denaturation could account for the observed difference in the CD spectra. This result is in good accordance with the pH effect observed on the OPH surface pressure−area isotherm. The LB film technique preserves the enzyme secondary structure with respect to the solution. For the temperature effect, the optimum temperature observed for the OPH solution is 20 °C. Far-UV CD spectra of OPH solid samples displayed no significant change in band shape or position over the temperature range from 20 to 60 °C; however, some variations in intensity were observed. The thermal stability of the OPH LB and dry films is much improved compared to that of the OPH solution, which is interpreted as being due to a close molecular arrangement of the enzyme. This indicates that the secondary structure of OPH can be stabilized when it is immobilized as LB or dry films. These results are very promising for development of OPH biosensors used for the environmental monitoring of organophosphorus compounds.

Acknowledgment. This work was supported by a grant from the U.S. Army Research Office (DAAD 19-03-1-0131). We thank the referee who reviewed the manuscript for his useful comments.

References and Notes

(1) Karalliedde, L. *Anaesthesia* **1999**, *54*, 1073−1088.
(2) Singh, A. K.; Flounders, A. W.; Volponi, J. V.; Ashley, C. S.; Wally, K.; Schoeniger, J. S. *Biosens. Bioelectron.* **1999**, *14*, 703−713.
(3) Dumas, D. P.; Wild, J. R.; Raushel, F. M. *Biotechnol. Appl. Biochem.* **1989**, *11*, 235−243.
(4) Dumas, D. P.; Caldwell, S. R.; Wild, J. R.; Raushel, F. M. *J. Biol. Chem.* **1989**, *33*, 19659−19665.
(5) Dumas, D. P.; Durst, H. D.; Landis, W. G.; Raushel, F. M.; Wild, J. R. *Arch. Biochem. Biophys.* **1990**, *227*, 155−159.
(6) Munnecke, D. M. *J. Agric. Food Chem.* **1980**, *28*, 105−111.
(7) Rogers, K. R.; Wang, Y.; Mulchandani, A.; Mulchandani, P.; Chen, W. *Biotechnol. Prog.* **1999**, *15*, 517−521.
(8) Mello, S. V.; Coutures, C.; Cheng, T. C.; Rastogi, V. P.; DeFrank, J. J.; Leblanc, R. M. *Talanta* **2001**, *55*, 881−887.
(9) Constantine, C. A.; Gattas-Asfura K. M.; Mellow, S. V.; Crespo, G.; Rastogi, V.; Cheng, T. C.; DeFrank, J. J.; Leblanc, R. M. *Langmuir* **2003**, *19*, 9863−9867.
(10) Constantine, C. A.; Mello, S. V.; Dupont, A.; Cao, X. H.; Santos, D.; Oliveira O. N.; Strixino, F. T.; Pereira, E. C.; Cheng, T. C.; DeFrank, J. J.; Leblanc, R. M. *J. Am. Chem. Soc.* **2003**, *125*, 1805−1809.
(11) Constantine, C. A.; Gattas-Asfura, K. M.; Mello, S. V.; Crespo, G.; Rastogi, V.; Cheng, T. C.; DeFrank, J. J.; Leblanc, R. M. *J. Phys. Chem. B* **2003**, *107*, 13762−13764.
(12) Serizawa, T.; Hashiguchi, S.; Akashi, M. *Langmuir* **1999**, *15*, 5363−5368.
(13) Wang, J.; Lin, Y. H.; Eremenko, A. V.; Kurochkin, I. N.; Mineyeva, M. F. *Anal. Chem.* **1993**, *65*, 513−516.
(14) Eremenko, A.; Kurochkin, I.; Chernov, S.; Barmin, A.; Yaroslavov, A.; Moskvitina, T. *Thin Solid Films* **1995**, *260*, 212−216.
(15) Cao, X.; Mello, S. V.; Sui, G.; Mabrouki, M.; Rastogi, V. K.; Cheng, T. C.; DeFrank, J. J.; Leblanc, R. M. *Langmuir* **2002**, *18*, 7616−7622.
(16) Sreerama, N.; Venyaminov, S. Y.; Woody, R. W. *Anal. Biochem.* **2000**, *287*, 243−251.
(17) Sreerama, N.; Woody, R. W. *Anal. Biochem.* **2000**, *287*, 252−260.
(18) Hirst, J. D.; Colella, K.; Gilbert, A. T. B. *J. Phys. Chem. B* **2003**, *107*, 11813−11819.
(19) Brahms, S.; Brahms, J. *J. Mol. Biol.* **1980**, *138*, 149−178.
(20) Hennessey, J. P.; Johnson, W. C. *Biochemistry* **1981**, *20*, 1085−1094.
(21) Wu, H.; Fan, Y.; Sheng, J.; Sui, S. *Eur. Biophys. J.* **1993**, *22*, 201−205.
(22) Erokhin, V.; Facci, P.; Kononenko, A.; Radicchi, G.; Nicolini, C. *Thin Solid Films* **1996**, *284−285*, 805−808.
(23) Pretzer, D.; Schulteis, B. S.; Smith, C. D.; Vander Velde, D. G.; Mitchell, J. W.; Manning, M. C. *Pharm. Res.* **1991**, *8*, 1103−1112.
(24) Shimizu, M.; Kobayashi, K.; Morii, H.; Mitsui, K.; Knoll, W.; Nagamune, T. *Biochem. Biophys. Res. Commun.* **2003**, *310*, 606−611.
(25) Greenfield, N. J. *Anal. Biochem.* **1995**, *235*, 1−10.
(26) Sreerama, N.; Woody, R. W. *Anal. Biochem.* **1993**, *209*, 32−44.
(27) Sreerama, N.; Woody, R. W. *Biochemistry* **1994**, *33*, 10022−10025.
(28) Sreerama, N.; Woody, R. W. *J. Mol. Biol.* **1994**, *242*, 497−507.
(29) Zimmerman, S.; Scheraga, H. P. *Natl. Acad. Sci. U.S.A.* **1977**, *74*, 4126−4129.